Biointerface Research in Applied Chemistry
Platinum Open Access Journal (ISSN: 2069-5837)

Article
Volume 14, Issue 6, 2024, 142
https://doi.org/10.33263/BRIAC146.142

Corrosion Inhibition of Expired Dogmatil Drug on Carbon Steel in HCl Solution: Experimental and Theoretical Approaches

Dalia N. Nasr [1], Ahmed El-Hossiany [1,2], Mai A. Khaled [3], Aya M. Salem [4], Abd El-Aziz S. Fouda [1,*]

[1] Department of Chemistry, Faculty of Science, Mansoura University, Mansoura 35516, Egypt
[2] Delta Fertilizers Company on Talkha, Egypt
[3] Department of Basic Science, Faculty of Engineering, Horus University, New Damietta, Egypt
[4] Higher Institute of Electronic Engineering (HIEE), Department of Basic Science, Belbis, Egypt
* Correspondence: asfouda@mans.edu.eg;

Scopus Author ID 56231506400
Received: 18.06.2024; Accepted: 6.10.2024; Published: 12.12.2024

Abstract: This study demonstrates the use of several methods to suppress corrosion as well as the use of an expired medication termed expired Dogmatil drug (EDD), which functions as a corrosion inhibitor for CS in 1M HCl. In this case, an analysis using weight loss (WL) and electrochemical measurements was conducted. At 150 ppm and 318 K, EDD produced an inhibitory efficiency (IE) of 98.3%. The %IE rises with increasing drug dose and solution temperature. The EDD adsorption on the CS surface followed the Langmuir adsorption isotherm. Furthermore, because EDD operates on both anodic and cathodic processes, it unifies its many protective qualities, making it a mixed-type inhibitor. The computed thermodynamic and activation parameters were examined in order to gain a deeper understanding of the inhibitive process. The computational results showed that the drug prevented CS from corroding by forming a barrier that protected it from acid attack. The experimental findings were supported by these validated outcomes. Fourier-transform infrared spectroscopy (FTIR) analysis, atomic force microscopy (AFM), energy-dispersive X-ray (EDX), and scanning electron microscopy (SEM) all support this adsorption. Both the chemical and electrochemical measurement results show good agreement with one another.

Keywords: corrosion inhibition; expired dogmatil drug; carbon steel; HCl; Langmuir isotherm.

1. Introduction

Corrosion is a dangerous weapon that affects not only metals but also plants, animals, environments, and human health. Its definition is the interactions between the metal and its environment. If metals are subjected to corrosion, they will liberate toxins into the air and water, which cause pollution to the environment and threaten human health. However, metals tend to corrode to retain their natural form, called ore, which is a thermodynamically stable form. Expired drugs are used to recycle many pharmaceutically active substances and are called pharmaceutical compounds [1]. These pharmaceutical compounds lead to reduced cost and environmental pollution, and they have other benefits such as high solubility, large molecular weight, and benign nature, so they are recommended for use instead of organic inhibitors, which are dangerous and expensive [2]. Expired drugs have chemical structures that contain many donating atoms, which make them good corrosion inhibitors. Increasing the number of donating atoms will increase the inhibition of corrosion. For this reason, using expired drugs

is the perfect choice for corrosion inhibition. In this research, we use Dogmatil as a corrosion inhibitor of CS in 1M HCl. Firstly, our Dogmatil drug (EDD) appeared for the first time in 1976 in published literature, and its primary use in medicine is the treatment of acute and chronic schizophrenia [3, 4]. EDD is considered a neuroleptic and antidepressant. EDD has a great effect on the nervous system, so doctors recommend it in cases of depression and irritable bowel syndrome. It must be used at the dose prescribed by a doctor to avoid its side effects, such as hyperprolactinemia and premature dyskinesia. It is an organic molecule that prevents corrosion by using an adsorption technique on the surface of metal by blocking its active site [5-7]. The occurrence key of the adsorption process is the chemical structure of EDD. It contains donating atoms such as oxygen, nitrogen, and sulfur in addition to benzene rings, which increase the inhibition process and influence the adsorption process by their lone pairs, which transfer into unoccupied d-orbitals of CS metal, leading to the formation of strong chemical bond which called a covalent bond. This chemical bond increases by increasing temperature. In this technique, EDD covers the space of the CS surface, forming a protective coating with a strong covalent bond [8-15]. Not only EDD is used for corrosion inhibition of CS in 1M HCl, but also many drugs are used for the same role as Phenytoin sodium drug (PSD) [16], Streptomycin [17], sulfa drugs compounds (e.g., sulfaguanidine, sulfamethazine, sulfamethoxazole and sulfadiazine) [18], green antihypertensive drug-Losartan potassium (LP) [19], Atenolol (ATL) and Nifedipine (NDP) [20], expired atorvastatin (EA) [21], Expired ranitidine [22], expired pantoprazole sodium EPS drug [23], Irbesartan [24], Cefalexin [25], Modazar [26], ampicillin [27], Tiazofurin [28], cloxacillin [29], Tetracycline [30], ciprofloxacin [31], 2-(2, 6-Dichloranilino) phenylacetic acid [32], Ketosulfone [33], and melatonin [34]. Finally, from the above, EDD can be seen as a corrosion inhibitor that keeps the surface of metal away from corrosion in 1M HCl. In this research, we will prove it through several techniques such as weight loss, EIS, AFM, FTIR, EDX, and SEM. After that, we will discuss how EDD can reduce the corrosion rate by using CS, whose main problem is its low resistance to corrosion in acidic medium, especially HCl and sulphuric acid solution, and it is more prone to corrosion than other steel types. CS is considered a type of iron alloy because iron is the main component, and at the same time, carbon is its most common element [35]. So, we can say that it has a mix of iron and carbon with different percentages. It contains other elements, such as sulfur, silicon, phosphorous, aluminum, and manganese, which can affect and change its properties. It has both mechanical and physical properties. Mechanical properties make it so popular as firmness and strength. On the other hand, physical properties as thermal conductivity and corrosion resistance. Thermal conductivity can be used to prevent cracking as a result of changing temperature. In brief, its versatility, its properties and its low price give it a great ability for many uses such as in medical instruments, industrial and engineering fields; any project needs strong and durable product, refining, components of bridges, chemical processing, petroleum production, steel piping and automotive parts [36, 37]. Acid solution, which is HCl, is used in washing of boilers, pickling to reduce scale, acid cleaning and descaling, components of rockets, purification, pH control as well as oil and petrochemical industries [38].

2. Materials and Methods

2.1. Materials and solution.

The metal used in our research is carbon steel. It is composed of several elements, as shown in the following Table.

Table 1. The chemical composition of CS (wt %).

Element	C	Mn	P	Si	Fe
Weight %	0.20	0.60	0.04	0.003	The rest

The experimental measurements were carried out in one molar HCl solution with and without various doses of EDD.

2.2. Inhibitors preparation.

EDD needs primarily some preparation before using 1000 mg of it is only needed. It was prepared by grinding five tablets with the highest concentration, 200 mg, to reach the desired concentration. After that, it was dissolved with distilled water. Then, it is used as stock to prepare several doses, which are needed in our research, using the dilution technique (25, 50, 75, 100, 125, 150 ppm). Its chemical structure is shown in Figure (1); its chemical formula is $C_{15}H_{23}N_3O_4S$, and its molecular weight is 341.427 g/mol.

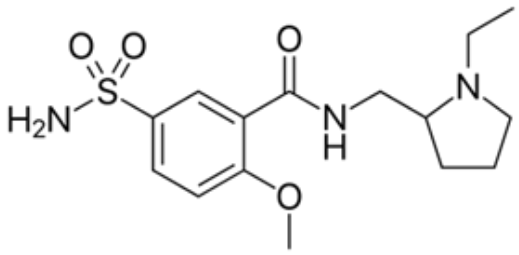

Figure 1. Chemical structure of EDD.

2.3. WL method.

It is a highly accurate and precise method for determining the inhibition efficiency and metal corrosion rate. It is a very simple method. "For doing it, seven identical CS samples are needed; their dimensions are 2×2×2 cm, and their surface areas are 8 cm^2. Firstly, these samples must be abraded by different grades of abrasive papers". Then, wash them with dist water and weigh them. After that, immersed in 1M HCl with and without different doses of inhibitor, which are included (25, 50, 75, 100, 125, 150 ppm). This experiment lasted for only three hours. At equal time intervals, i.e., 30 min., samples are taken and ejected from acidic solutions and reweighted. Finally, the θ)following equations can calculate the surface coverage degree (θ and % IE). [39-40,26]:

$$\theta = (w_0 - w_{inh})/\, w_0 \qquad (1)$$

$$\%\, IE = \left[\frac{w_0 - w_{inh}}{w_0}\right] \times 100 \qquad (2)$$

Where w_o and $w_{inh} w_0$ $and\ w_{inh}$ are the values of WL with and without the addition of EDD.

2.4. Electrochemical methods.

They include several techniques, such as EIS and PDP. These techniques are used to prove the results of the mass loss method. Many types of electrodes are applied for them, such

as the reference electrode, a saturated calomel electrode SCE, platinum as an auxiliary electrode, and the working electrode. The working electrode is a CS sample with two sides. One is exposed to the test solution, and the other is welded with a CS rod [41]. To determine the steady state open circuit potential (OCP), the samples were submerged in a one-molar HCl solution for 30 minutes at room temperature. A potential scan between –250 and +250 mV was performed at 1 mVs^{-1} in order to identify polarization. The EIS results have been achieved with an amplitude of 10 mV over a frequency range of 0.01 Hz to 10 kHz. The solutions were not aerated; all tests were conducted at 298 K with a circulator. Every test was conducted using a newly made electrolyte and an electrode that had just been cleansed. The %IE was determined using Eqs. (3 & 4) based on the results of the PDP and EIS, respectively:

$$\%IE_{PDP} = \left(1 - \frac{i_{corr}}{i^{\circ}_{corr}}\right) \times 100 \quad (3)$$

$$IE_{EIS} = \left(1 - \frac{R^{\circ}_{ct}}{R_{ct}}\right) \times 100 \quad (4)$$

Where i^{o}_{corr} and i_{corr} represent the corrosion current densities of the samples exposed to the HCl solution and the electrolyte shielded by EDD, the resistance associated with charge transfer in the presence and absence of EDD is represented by the parameters of R^{o}_{ct} and R_{ct}, in a similar manner.

2.5. Surface analysis.

2.5.1. FTIR technique.

It is used to determine the functional groups that are present in EDD by adding the highest concentration of it in 1M HCl in the presence of CS for about three hours.

2.5.2. AFM technique.

It is used to detect the morphological characteristics of CS's outer surface, which becomes rough because its ideal shape deviates from its ideal shape due to the occurrence of corrosion or inhibitor adsorption. This technique is performed by adding CS metal in 1M HCl in the presence and absence of EDD for also three hours. At the same time, one of the CS metals was taken as a free reference, which means that it is not subjected to either inhibitor or HCl.

2.5.3. SEM-EDX analysis.

These measurements use JEOL JSM-5500. This technique is most likely to AFM as it is also used to identify the morphological characters of CS's outer surface. Nearly the same steps of the AFM technique are done by dipping CS metal in 1M HCl, and there is a lack of maximum EDD for three hours.

2.6. Theoretical calculations.

It is considered one of the most important theoretical tools that is used to illustrate the interaction between EDD inhibitors on the CS surface. There are a lot of parameters derived from it, such as total energy, “adsorption energy, rigid adsorption energy, and deformation energy” [42-44].

3. Results and Discussion

3.1. WL tests.

Following a series of dips (30, 60, 90, 120, 150, and 180 min) at varying temperatures (298, 303, 308, 313, and 318 K) in one molar HCl with and without EDD, the WL measurements of the CS samples are computed and plotted against time to produce a graph of Figure 2. In this graph, WL-time curves at 298 K are explained. This graph demonstrates how WL drops when an inhibitor is present. Table 2 illustrates that the percentage of corrosion inhibition (%IE) increases as the EDD dose increases due to temperature effects. This is because EDD coats a significant portion of the CS surface and creates a protective film, significantly reducing corrosion [40, 45].

Table 2. θ, and %IE of EDD with altered doses of EDD under the effect of temperature for corrosion inhibition of CS after 120 min immersion in one molar HCl.

Conc., ppm	298 K		303 K		308 K		313 K		318 K	
	θ	%IE	θ	%IE	θ	%IE	θ	%IE	θ	%IE
25	0.892	89.2	0.950	95.0	0.960	96.0	0.965	96.5	0.965	96.5
50	0.903	90.3	0.956	95.6	0.965	96.5	0.971	97.1	0.973	97.3
75	0.915	91.5	0.960	96.0	0.970	97.0	0.974	97.4	0.976	97.6
100	0.918	91.8	0.961	96.1	0.970	97.0	0.975	97.5	0.977	97.7
125	0.922	92.2	0.964	96.4	0.972	97.2	0.977	97.7	0.978	97.8

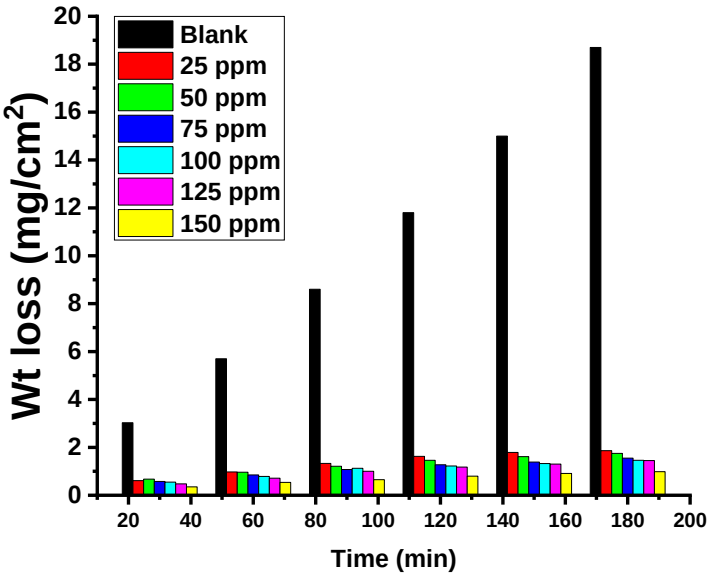

Figure 2. Shows the WL-time curves for the corrosion of CS in one molar HCl both with and without changed EDD dosages at 298 K.

3.1.1. Adsorption isotherm.

The adsorption process is performed as a substitution process as the adsorbed water molecule is replaced by an inhibitor molecule on the surface of CS metal [46, 47].

$$Inh_{(sol)} + nH_2O \rightarrow Inh_{(ads)} + H_2O_{(ads)} \quad (5)$$

To clarify this mechanism, several isotherms are used, such as Langmuir, Frumkin, Temkin, and Freundlich isotherms. The Langmuir is the best fit to characterize the adsorption technique. Figure 3 shows Langmuir isotherm, which is given by formula [48, 49]:

$$C_{inh}/\theta = (1/K_{ads}) + C_{inh} \quad (6)$$

Kads is the adsorption equilibrium constant, θ is the surface covering degree, and C_{inh} is the inhibitor dose. The Langmuir isotherm is the most appropriate to describe the adsorption of EDD inhibitor on the CS surface, as shown by the plotting of C_{inh}/θ against C_{inh}, which

results in a straight line with a slope that approaches one, an intercept equal to ($1/K_{ads}$), and a correlation coefficient (R^2) that is almost equal to unity [50].

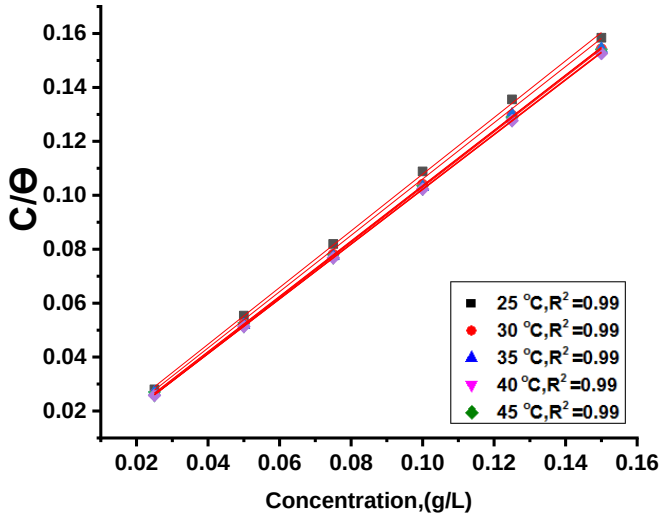

Figure 3. Langmuir adsorption of EDD on CS surface in 1 M HCl at different temperatures.

Adsorption free energy ΔG^{o}_{ads}, which may be computed using the following equation [51–53], is related to K_{ads}:

$$K_{ads} = \frac{1}{55.5} \times \exp\left(-\frac{\Delta G^{\circ}_{ads}}{RT}\right) \quad (7)$$

Where T is the absolute temperature, R is the universal gas constant, and the molar concentration of water in solution is 55.5.

With the value of ΔG^{o}_{ads} known, the kind of adsorption may be identified right away. Adsorption can be chemical or physical. The value of ΔG^{o}_{ads} for chemisorption is around -40 kJ mol^{-1} or more, whereas the value for physisorption is approximately -20 kJ mol^{-1} or below [54–58]. The spontaneous nature of the adsorption process is demonstrated by the negative (-ve) value of ΔG^{o}_{ads}. The enthalpy (ΔH^{o}_{ads}) can be computed from the slope, which is equal to -(ΔH°_{ads})/(2.303×R), after graphing log K_{ads} vs. 1000/T (Fig. 4).

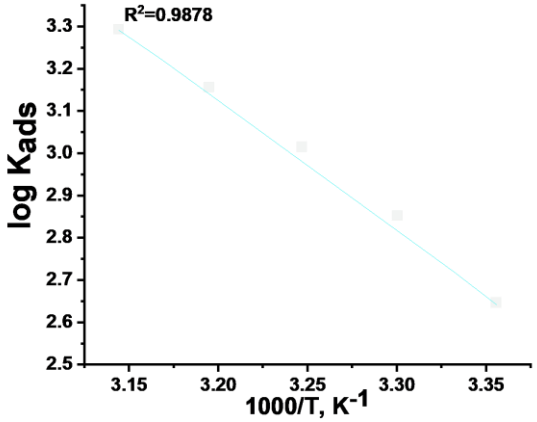

Figure 4. Log K_{ads} vs. 1000/T for the corrosion of CS in one molar HCl.

ΔH^{o}_{ads} can be either positive or negative. In case of a negative value, the adsorption process is exothermic and might be either physical or chemical [59]. Conversely, if the value is positive, the adsorption will be chemical in nature, and the process will be endothermic [60]. Lastly, the following equation [61] computes the adsorption entropy (ΔS^{o}_{ads}):

$$\Delta G^{\circ}_{ads} = \Delta H^{\circ}_{ads} - T\Delta S^{\circ}_{ads} \quad (8)$$

Table 3 presents essential thermodynamic parameters of the adsorption of ED inhibitor on the CS surface. From the data, the value of ΔG^{o}_{ads} is around 30 kJ mol^{-1}, and this indicates that the type of adsorption is mixed type, i.e., physical and chemical. Still, in our research, adsorption is mainly chemisorption due to many reasons. The first reason is the positive value of (ΔH^{o}_{ads}), which confirms that adsorption is chemisorption and the endothermic reaction [62]. The second one is that the activation energy (E*a) decreases in the presence of ED rather than in its absence, and it also decreases by increasing its concentration. The last reason is the percentage of % IE rises to rise of temperature.

Table 3. Langmuir adsorption parameters at different temperatures.

Temp. K	Log K_{ads} (M^{-1})	$-\Delta G^{o}_{ads}$ (kJ mol^{-1})	$-\Delta H^{o}_{ads}$ (kJ mol^{-1})	ΔS^{o}_{ads} (J mol^{-1} K^{-1})
298	2.6	24.6	58.7	279.6
303	3.0	27.5		284.7
308	3.1	28.1		281.8
313	3.2	29.7		282.7
318	3.3	30.4		280.4

The positivity of ΔS^{o}_{ads} indicates increased randomness at the metal surface due to the desorption of the H_2O molecule and strong adsorption of inhibitor during the adsorption mechanism [63].

3.1.2. Effect of temperature.

The effectiveness of temperature on the corrosion rate of CS in 1M HCl using various doses of EDD inhibitor, which are between 25 and 150 ppm, can be checked by a WL test. Several temperatures ranging from 298 to 318 K are used. As shown in Table 2, the %IE of EDD increases with increasing temperature, which means that the adsorption type is undoubtedly chemisorption. The activation energy (E^{*}_{a}) can be calculated using the Arrhenius equation [64].

$$k_{corr} = A\ exp\left(-\frac{E^{*}_{a}}{RT}\right) \qquad (9)$$

Where A is the Arrhenius constant, k_{corr} is the corrosion rate, R is the general gas constant, and T is the absolute temperature. In Figure 5, plotting Log k_{corr} against 1000/T exhibits a straight line, so E^{*}_{a} can be obtained from the slopes of the graph, which equals ($-E^{*}_{a}$ / 2.303 R).

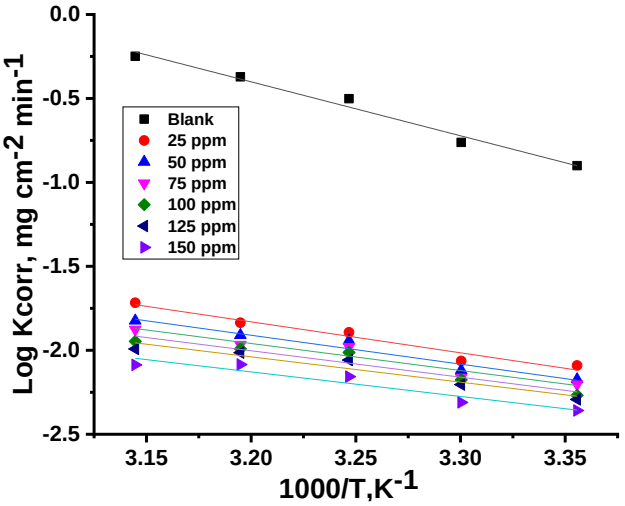

Figure 5. Arrhenius plots for CS corrosion rates (k_{corr}) after 120 minutes of dipping in one molar HCl with and without altered doses of EDD.

By applying the transition state theory, the enthalpy (ΔH^*) and entropy (ΔS^*) are calculated by the given equation [65]:

$$k_{corr} = "(RT/Nh)\ \exp(\Delta S^*/R)\ \exp(-\Delta H^*/RT)" \quad (10)$$

Where h represents Planck's constant, N represents Avogadro's number, ΔS^* represents activation entropy, and ΔH^* represents activation enthalpy.

After that, Figure 6 illustrates the plotting of log k_{corr}/T vs. 1000/T, which also shows a straight line, and the activation enthalpy and entropy can be determined from slope and intercept, respectively. The slope equals to $(\Delta H^*/2.303R)$, and the intercept equals to $[\log(R/Nh) + \Delta S^*/2.303R)]$ [66]. The activation parameters are depicted in Table 4.

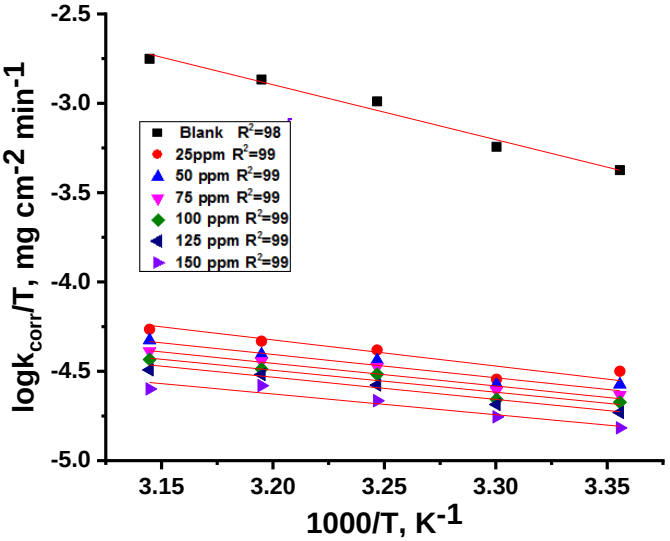

Figure 6. Transition state CS corrosion rates (k_{corr}) in one molar HCl in the presence and absence of various doses of EDD.

Table 4. Depict the values of E^*_a, ΔH^*, and ΔS^*.

Conc., ppm	Activation parameters		
	E^*_a, kJ mol.$^{-1}$	ΔH^*, kJ mol.$^{-1}$	$-\Delta S^*$, J mol.$^{-1}$K^{-1}
Blank	41.5	39.3	195.6
25	32.8	30.4	201.6
50	30.9	28.4	205.1
75	28.9	26.3	206.9
100	28.7	25.9	208.2
125	27.4	24.7	209.6
150	26.3	23.1	214.9

As seen from Table 4, the E^*_a decreases by increasing the temperature and concentration of the inhibitor, which indicates that the type of adsorption of EDD on CS is chemical. Also, the values of ΔS^* are large and negative, which explains that activated complex tends to exist in the association phase instead of the dissociation step [67].

3.2. Electrochemical analysis.

3.2.1. PDP measurements.

Figure 7 demonstrates the Tafel polarization diagrams. It includes both anodic metal dissolution and cathodic H_2 reduction in the presence and absence of different doses of EDD in one molar HCl. There are several electrochemical parameters, including corrosion potential (E_{corr}), anodic and cathodic slopes (β_a, β_c), and corrosion current (i_{corr}), which shows a significant decrease after the addition of EDD with increasing its dose (Table 5). E_{corr} is slightly changed, and its value is less than ±85; and this illustrates that EDD is a mixed-type inhibitor.

The reaction mechanism is not altered because Tafel slopes (βa, βc) are constant and parallel Tafel lines, which are given in the presence and absence of EDD [68, 69].

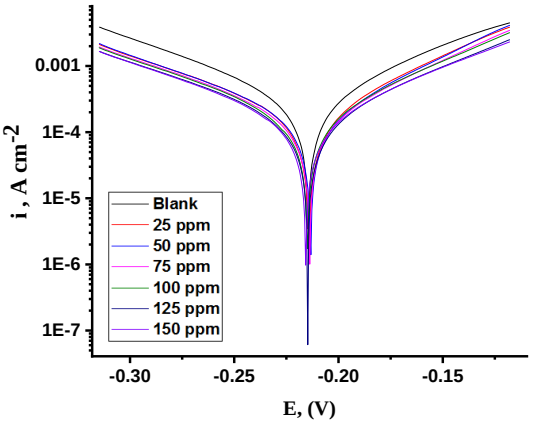

Figure 7. Tafel polarization curves of CS dissolution with and without altered doses of EDD at 25ºC.

Table 5. Corrosion parameters for CS in one molar HCl with various EDD doses.

Conc., ppm	$i_{corr.}$ (μA cm^{-2})	-$E_{corr.}$ (mVvs SCE)	β_a (mV dec^{-1})	-β_c (mV dec^{-1})	k_{corr} (mmy^{-1})	θ	% IE
Blank	995	218	79	110	148	--	--
25	194	217	69	101	34	0.805	80.5
50	185	219	79	103	30	0.814	81.4
75	135	215	80	107	28	0.864	86.4
100	128	216	88	104	27	0.871	87.1
125	117	214	73	112	25	0.882	88.2
150	94	217	88	106	21	0.906	90.6

3.2.3. EIS measurements.

It includes both Nyquist and Bode plots. Nyquist diagram shows a semicircle, which indicates that charge transfer occurred through the corrosion process (Figures 8 and 9).

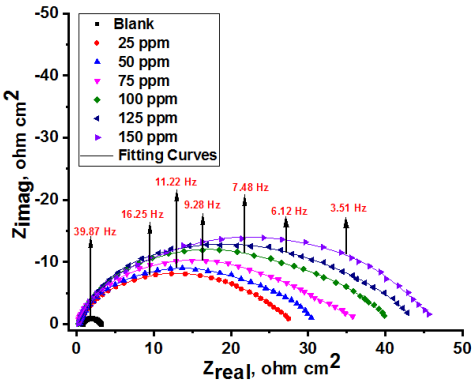

Figure 8. The Nyquist curves for CS dissolution in one molar HCl with and without different doses of EDD at 25°C.

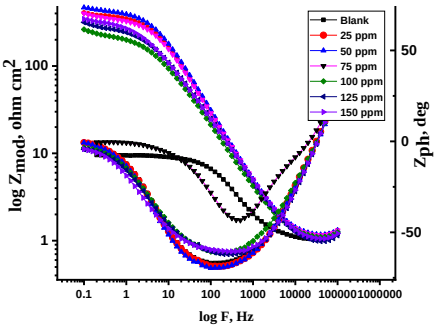

Figure 9. Bode curves for CS corrosion in one molar HCl in the absence and presence of altered doses of EDD at 25°C.

Nonperfect semicircles are displayed due to impurities, surface roughness, heterogeneous electrode surface, and inhibitor adsorption forming a porous layer, and the electrode surface becomes uniform. In the Bode plots, increasing the EDD dosages will increase both the absolute impedance at low frequencies and the electrode impedance response of CS in one molar HCl, both with and without an EDD inhibitor. Figure 8 shows the perfect fitting for CS in one molar HCl. R_S, R_{ct}, and C_{dl} are components of this electrical equivalent circuit (Figure 10).

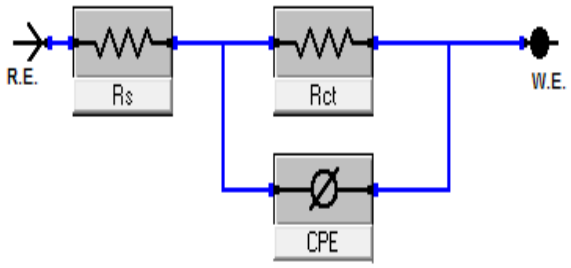

Figure 10. electrical circuits for experimental data fitting.

From the experimental data, it was found that an increase in EDD dose results in an increase in R_{ct} values and a decrease in C_{dl} values (Table 6). This idea resulted from water molecules desorbing and being replaced on the CS surface by EDD molecules. Ultimately, its capacity to reduce surface heterogeneity increases inhibitor efficiency with increasing EDD dosages [70]. C_{dl} is computed using the equation [71] below:

$$C_{dl} = Y^{\circ}(w_{max})^{n-1} \quad (11)$$

Where Y°CPE coefficient, w is the maximum frequency, and n is the CPE exponent. Figure 10. Fitting the impedance spectral data using the electrical equivalent circuit. Where R_s is the solution resistance between CS and reference electrode, and CPE is the charge phase element.

Table 6. EIS parameters for CS after dipping in one molar HCl in the existence of various EDD doses at 25°C.

Conc. (M)	Y_o, ($\mu\ \Omega^{-1}\ s^n\ cm^{-2}$) x$10^{-6}$	n	R_{ct}, $\Omega\ cm^2$	C_{dl}, $\mu F\ cm^{-2}$	Θ	IE %	Goodness of Fit χ^2
Blank	465	0.991	3.2	439	--	--	17.06x10^{-3}
25	362	0.989	29.9	344	0.893	89.3	13.22x10^{-3}
50	360	0.976	31.1	325	0.897	89.7	12.91x10^{-3}
75	335	0.942	37.7	256	0.915	91.5	11.31x10^{-3}
100	325	0.911	39.9	212	0.920	92.0	14.12x10^{-3}
125	310	0.901	42.2	192	0.924	92.4	16.19x10^{-3}
150	298	0.899	43.1	183	0.926	92.6	14.83x10^{-3}

3.3. Surface examination.

3.3.1. AFM Analysis.

It is an amazing method for describing the three-dimensional morphology of the CS outer surface. Three CS types are depicted in the following Figure 11. The first one is known as blank and is submerged in just one molar HCl. The second one is submerged in one molar HCl as well, but 150 ppm of EDD inhibitor is present. The last image illustrates free CS, which is not exposed to either HCl or inhibitor. Blank CS has significantly more damage than both other samples, so it has the highest mean roughness (S_a), which equals 211 nm. EDD inhibitor adsorbs on the CS outer surface, so the roughness obtained was reduced to 93.3 nm [72]. The free CS is clearer and has the lowest roughness, which equals 53 nm, and it is evidence that it is not affected by corrosion.

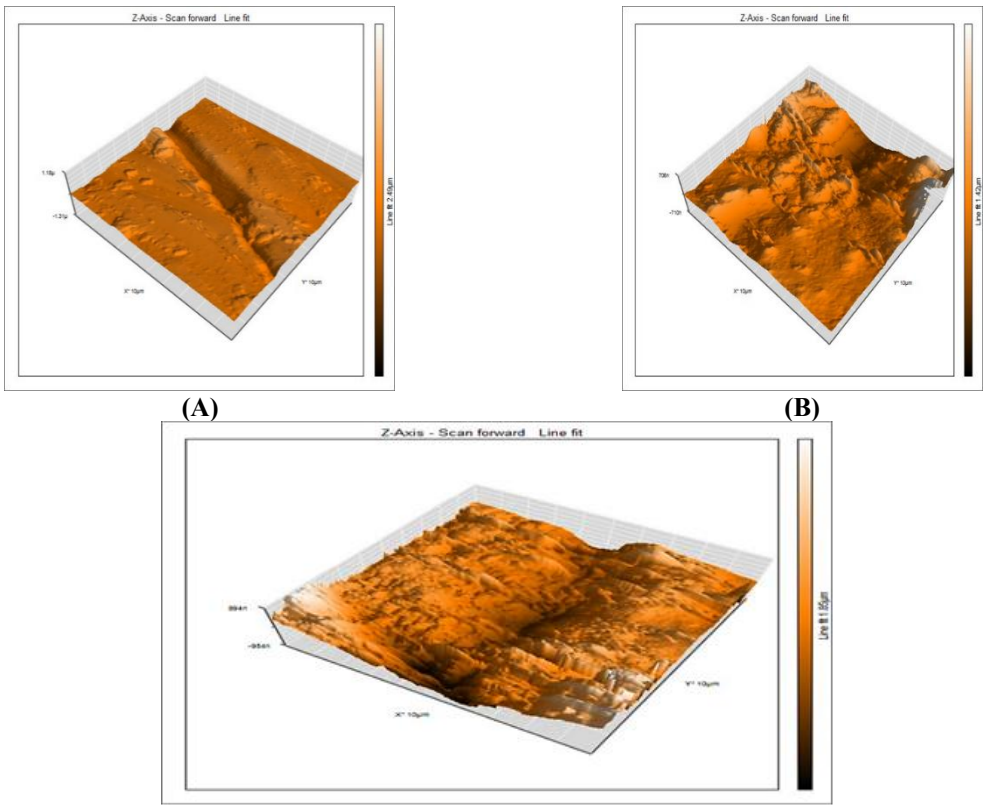

(A) **(B)**

(C)

Figure 11. AFM 3D images of **(A)** free CS smooth surface without any addition or immersion; **(B)** CS in one molar HCl only (Blank); **(C)** CS in one molar HCl + 150 ppm of EDD (within immersion for only 3 hours at 298 K).

3.3.2. SEM analysis.

It is an important technique used to confirm the efficiency of EDD inhibitors and their ability to adsorb and form a protective surface film on the CS surface. The CS surface was examined for only three hours in three cases, as shown in Figure 12. Firstly, Figure (12-A) presents the micrograph of the free CS surface without exposure to either HCl or inhibitor. Figure (12-B) illustrates that CS which is immersed in one molar HCl only. This image demonstrated that CS was severely degraded due to a very hard attack by corrosion and became rough and cracked. On the other hand, Figure 12-C shows that the CS surface smoothed out even after being dipped in a corrosive liquid with 150 ppm of EDD inhibitor present.

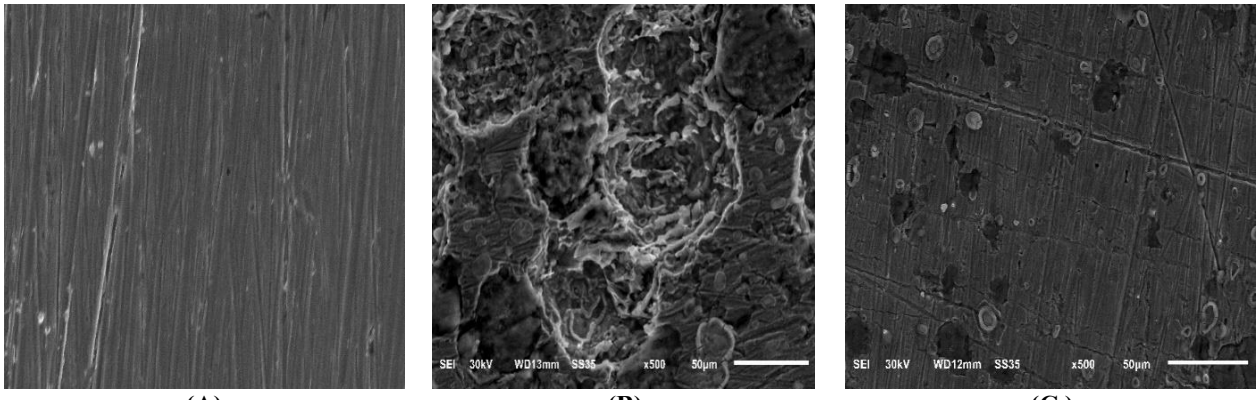

(A) **(B)** **(C)**

Figure 12. SEM images of **(A)** free CS; **(B)** CS after 3 hrs. dipped in one molar HCl only; **(C)** CS after 3 hrs. dipped in one molar HCl + 150 ppm of EDD.

This action of EDD inhibitor is due to its ability to adsorb on the CS surface and interact with reaction or active sites that are present on the CS surface, forming a protective coating on it and decreasing its contact with the corrosive medium [73]. From all the above, EDD is considered a perfect corrosion inhibitor.

3.3.3. EDX analysis.

The previous results were proved by the EDX technique. It is used to determine the percentage of elements present on the CS surface after immersion in a corrosive solution in the presence and absence of an inhibitor. Table 7 lists the composition of the CS surface of elements for all samples. Figure (13 A-C) shows the EDX profile analysis. Figure (13-A) explains the spectra of free CS with the highest concentration of iron as a strong Fe signal. In this case, CS is richer in iron than in any other case. Figure (13B) illustrates that CS is dipped in one molar HCl only. This spectrum indicates the presence of Cl obtained from the HCl medium and the formation of iron chloride, as well as the presence of the lowest concentration of iron and the highest concentration of oxygen due to the formation of iron oxides (Fe_2O_3 and Fe_3O_4), which considered evidence of corrosion occurrence [74,75]. Figure (13C) showed increasing in the iron more than the blank sample, which is related to the strong effect of the inhibitor and its %IE. The presence of oxygen is due to the oxygen atom of EDD.

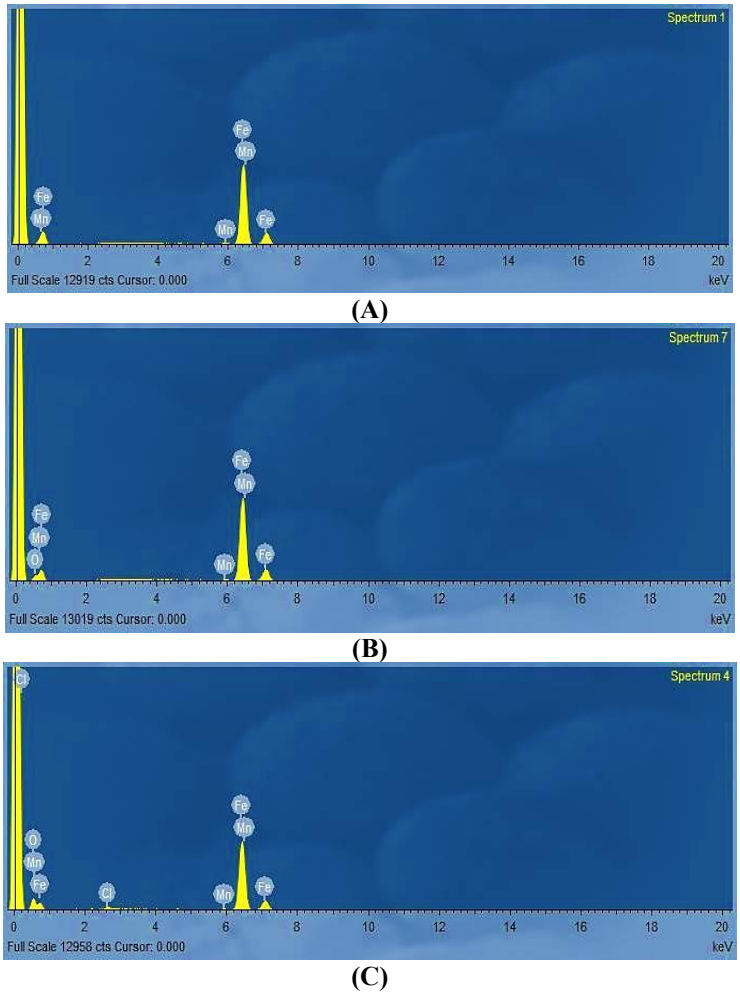

Figure 13. EDX spectra of **(A)** free CS; **(B)** CS after 3 hrs. dipping in 1 M HCl only; **(C)** CS after 3 hrs. dipping in 1M HCl + 150 ppm of EDD.

Table 7. Surface composition (mass %) of CS before and after 3 hours of exposure to corrosive acid medium without and with 150 ppm of EDD.

Samples	Mass %			
	Fe	O	Mn	Cl
Free CS	99.2	0.00	0.84	0.00
Blank	71.1	27.1	0.47	1.33
ED inhibitor	87.4	12.1	0.53	0.00

3.4. Theoretical calculations.

3.4.1. MC simulation.

Figure 14 shows the final equilibrium configuration obtained from the MC (side and top) view for EDD on the surface". Through the adsorption process, adsorption energy is either required or liberated [76].

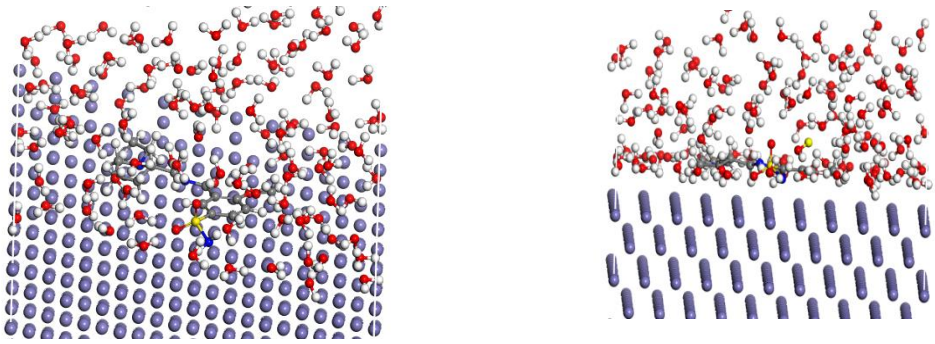

(a) **(b)**

Figure 14. Final equilibrium configuration obtained from MC **(a)** top; **(b)** side view for EDD on the surface.

The released energy is measured by deformation energy. Adsorption energy is characterized as declining energy and can be calculated by summation of both rigid adsorption energy and deformation energy, as shown in Table 8 [77]. A negative value of adsorption energy indicates the stability of EDD adsorption on the CS surface. By decreasing the adsorption energy, the inhibitor's adsorption affinity and inhibition efficiency will be high (Table 8). The adsorption locator module is used to describe the top and side view of the most suitable, stable, and lowest energy configuration for the adsorption of EDD on the CS surface. The side view indicates that EDD is parallel to the surface of CS, but the top view shows that EDD is nearly flat on the CS surface. This means that the CS surface is already covered with EDD inhibitor, which creates an adsorbed stable layer to protect it from corrosion.

Table 8. MC emulation variables of EDD molecule on Fe (1 1 0).

Structure	Total energy	Adsorption energy	Rigid adsorption energy	Deformation energy	E_{ads}: compound
1 1 0) – 1EDD	-3393.897	-3326.192	-3497.692	171.5	-234.27

3.4.2. Quantum chemical calculation.

Figure 15 shows the frontier molecular provides the electron density maps of HOMO and LUMO for the EDD. DFT theory is applied to quantify the EDD molecule's quantum chemical properties.

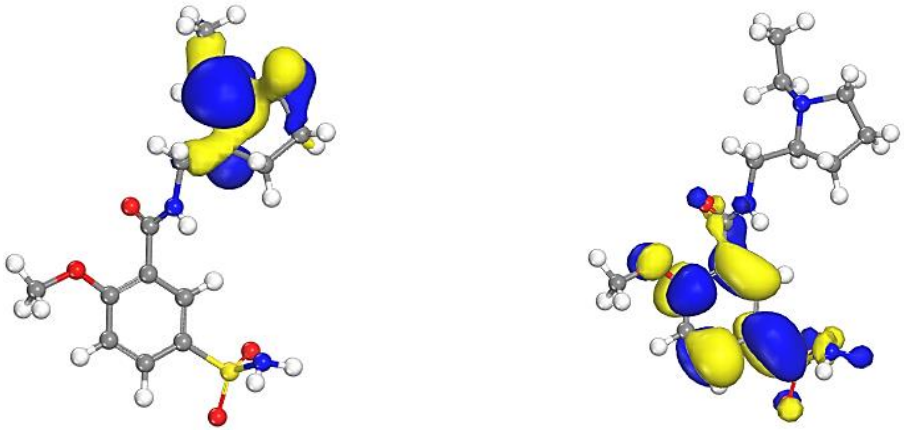

(a) **(b)**

Figure 15. The frontier molecular provides the electron density maps of **(a)** HOMO; **(b)** LUMO for the EDD.

The relationship between the CS surface and EDD was influenced by these characteristics. These include highest occupied molecular orbital (E_{HOMO}), lowest unoccupied molecular orbital (E_{LUMO}, dipole moment (μ), energy gap (ΔE), electron affinity (A), ionization potential(I), electronegativity (χ), global hardness (η) and softness (σ) (Table 9). Firstly, E_{HOMO} illustrates the ability of the inhibitor to donate electrons to the empty d-orbital which is present on the CS surface. By increasing its value, the %IE will increase, and the adsorption process will be more facilitated and become easier [78]. On the other hand, E_{LUMO} indicates the tendency of molecules to accept electrons. Reducing the value of ELUMO will boost a molecule's capacity to receive electrons. Since ΔE represents the energy required to remove an electron from the final occupied orbital, it was deemed desirable to be low.

This equation is used to calculate it:

$$\Delta E = E_{LUMO} - E_{HOMO} \quad (12)$$

Additionally, as it creates a connection between the ionization potential and the electron affinity, A and I are connected to the E_{HOMO} and the E_{LUMO}. The absolute electronegativity, χ, and hardness, η, respectively, Equations following illustrate the calculation of the inhibitor molecule's global softness, σ.

$$I = -E_{HOMO} \quad (13)$$

$$A = -E_{LUMO} \quad (14)$$

$$\chi = \frac{I+A}{2} = -\frac{E_{HOMO}+E_{LUMO}}{2} \quad (15)$$

$$\eta = \frac{I-A}{2} = \frac{E_{LUMO}-E_{HOMO}}{2} = \frac{1}{2}\Delta E_{L-H} \quad (16)$$

$$\sigma = \frac{1}{\eta} \quad (17)$$

The lower value ΔE will render the reactivity and inhibition efficiency of EDD high and strong [79]. Dipole moment (μ) improves the adsorption of EDD on CS surface by increasing its value". As a result, the strong dipole-dipole connections between the inhibitor and the metal surface, as demonstrated in Table 9, are responsible for the inhibitor's high dipole moment. Certain parameters, such as global hardness (η) and softness (σ), are linked to the molecule's selectivity and reactivity. As per the Lewis theory of acid/base and Pearson's hard/soft acids and bases [80], more reactive and bigger ΔE values are associated with hard molecules. Based on Table 9, it can be inferred that EDD has a greater σ value, indicating a softer nature. EDD would, therefore, be more likely to provide electrons to CS. If the ΔN value

of the inhibitor is higher, it is found to have a stronger capability of donating electrons to metallic surfaces [81].

Table 9. Quantum calculation parameters for a molecule of EDD obtained from DFT.

Parameters (Variable)	DFT
-E_{HOMO} (ev)	4.297
-E_{LUMO} (ev)	4.025
ΔE, (eV) (E_L-E_H)	0.27
μ (debye) (Dipole moment)	22.3
A (eV) (electron affinity)	4.025
I (eV) (ionization potential)	4.297
χ (eV) (electronegativity)	4.16
η (eV) (global hardness)	0.14
ΔN	10.44
σ (eV^{-1}) (softness)	7.35

3.5. Inhibition mechanism.

The EDD inhibitor can not start working or show its effect until it binds to the CS surface. This adsorption may be physical or chemical, so many parameters affect the adsorption process and degree of inhibition, such as metal surface and inhibitor charges, number of heteroatoms and aromatic ring, corrosive media composition, and the density of electrons [82]. Scheme 1 shows the adsorption of EDD on the CS surface. EDD is adsorbed chemically on the CS surface in a special way, which occurs by transferring unshared electrons of heteroatoms as well as benzene rings to the empty d-orbitals of iron atom on the CS surface, forming a complex between Fe and EDD inhibitor by coordination bonding. This behavior leads to forming a protective coating layer on the CS surface, which acts as a barrier to prevent its interaction with the corrosive environment. In this way, the CS surface is protected from corrosion [83,84]. On the other hand, protonated inhibitor molecules in 1 M HCl prefer physical adsorption through electrostatic interactions. They interact with negatively charged chloride ions, which are adsorbed on the CS surface. Finally, EDD has the potential to be a perfect corrosion inhibitor through the chemisorption process.

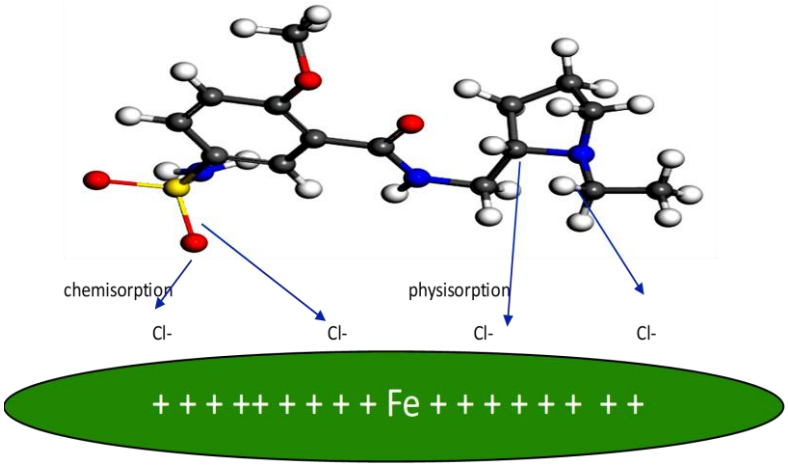

Scheme 1. Adsorption of EDD on CS surface.

4. Conclusions

The EDD acts as a good and efficient corrosion inhibitor for the corrosion of CS in 1M HCl solution. The IE increases with the temperature and the dose of the EDD. EDD's inhibition of CS corrosion can be attributed to the adsorption ability of its molecules onto the active sites of the metal surface. The adsorption of the EDD on the CS obeys Langmuir adsorption isotherm. Polarization data indicate that the EDD acts as a mixed-type inhibitor. SEM and AFM reveal the formation of a smooth, uniform surface on CS in the presence of the EDD, indicating a good protective layer on the metal surface. The results obtained from different measurements were consistent.

Funding

This research received no external funding.

Acknowledgments

We are grateful to the unknown referees for the attentive reading of the article and insightful comments that aided in creating this research into its current form. We would like to express our gratitude to the corrosion chemistry laboratory team at Mansoura University (Egypt) for their appreciative and respectful cooperation.

Conflicts of Interest

The authors declare no conflict of interest.

References

1. Montaser, A.A.; El-Mahdy, M.S.; Mahmoud, E.E.E.; Fouda, A.S. Recycling of expired ciprofloxacin in synthetic acid rain (SAR) solution as a green corrosion inhibitor for copper: a theoretical and experimental evaluation. *J. Appl. Electrochem.* **2024**, *54*, 439-456, https://doi.org/10.1007/s10800-023-01966-0.
2. Salem, A.M.; Wahba, A.M.; Hossiany, A.E.; Fouda, A.S. Experimental and computational chemical studies on the corrosion inhibitive properties of metamizole sodium pharmaceutical drug compound for CS in hydrochloric acid solutions. *Indian J. Chem.* **2022**, *99*, 100778, https://doi.org/10.1016/j.jics.2022.100778.
3. Justin-Besançon, L.; Thominet, M.; Laville, C.; Margarit, J. [Chemical consitution and biological properties of sulpiride]. *Comptes rendus hebdomadaires des seances de l'Academie des sciences. C. R. Acad. Hebd. Séances Acad. Sci. D.* **1967**, *265*, 1253-1254.
4. Mauri, M.C.; Bravin, S.; Bitetto, A.; Rudelli, R.; Invernizzi, G. A Risk-Benefit Assessment of Sulpiride in the Treatment of Schizophrenia. *Drug Saf.* **1996**, *14*, 288-298, https://doi.org/10.2165/00002018-199614050-00003.
5. Badr, E.A.; Bedair, M.A.; Shaban, S.M. Adsorption and performance assessment of some imine derivatives as mild steel corrosion inhibitors in 1.0 M HCl solution by chemical, electrochemical and computational methods. *Mater. Chem. Phys.* **2018**, *219*, 444-460, https://doi.org/10.1016/j.matchemphys.2018.08.041.
6. Bedair, M.A.; Soliman, S.A.; Metwally, M.S. Synthesis and characterization of some nonionic surfactants as corrosion inhibitors for steel in 1.0M HCl (Experimental and computational study). *J. Ind. Eng. Chem.* **2016**, *41*, 10-22, https://doi.org/10.1016/j.jiec.2016.07.005.
7. Elmorsi, M.A.; Hassanein, A.M. Corrosion inhibition of copper by heterocyclic compounds. *Corros. Sci.* **1999**, *41*, 2337-2352, https://doi.org/10.1016/S0010-938X(99)00061-X.
8. Al-Amiery, A.A.; Shaker, L.M. Corrosion inhibition of mild steel using novel pyridine derivative in 1 M hydrochloric acid. *KOM–Corrosion Mater. Protection J.* **2020**, *64*, 59-64, https://doi.org/10.2478/kom-2020-0009.
9. Alamiery, A.; Mahmoudi, E.; Allami, T. Corrosion inhibition of low-carbon steel in hydrochloric acid environment using a Schiff base derived from pyrrole: gravimetric and computational studies. *Int. J. Corros.*

Scale Inhib. **2021**, *10*, 749-765, http://dx.doi.org/10.17675/2305-6894-2021-10-2-17.
10. Alamiery, A.A. Anticorrosion effect of thiosemicarbazide derivative on mild steel in 1 M hydrochloric acid and 0.5 M sulfuric Acid: Gravimetrical and theoretical studies. *Materials Science for Energy Technologies* **2021**, *4*, 263-273, https://doi.org/10.1016/j.mset.2021.07.004.
11. Alkadir Aziz, I.A.; Annon, I.A.; Abdulkareem, M.H.; Hanoon, M.M.; Alkaabi, M.H.; Shaker, L.M.; Alamiery, A.A.; Wan Isahak, W.N.R.; Takriff, M.S. Insights into Corrosion Inhibition Behavior of a 5-Mercapto-1, 2, 4-triazole Derivative for Mild Steel in Hydrochloric Acid Solution: Experimental and DFT Studies. *Lubricants* **2021**, *9*, 122, https://doi.org/10.3390/lubricants9120122.
12. Kadhim, A.; Al-Amiery, A.A.; Alazawi, R.; Al-Ghezi, M.K.S.; Abass, R.H. Corrosion inhibitors. A review. *Int. J. Corros. Scale Inhib.* **2021**, *10*, 54-67, https://dx.doi.org/10.17675/2305-6894-2021-10-1-3.
13. Musa, A.Y.; Mohamad, A.B.; Al-Amiery, A.A.; Tien, L.T. Galvanic corrosion of aluminum alloy (Al2024) and copper in 1.0M hydrochloric acid solution. *Korean J. Chem. Eng.* **2012**, *29*, 818-822, https://doi.org/10.1007/s11814-011-0233-z.
14. Bozdogan, A.; Yasar, K.; Soyler, M.; Ozalp, C. Rheological Behavior of Sumac (*Rhus Coriaria* L.) Extract as Affected by Temperature and Concentration and Investigation of Flow Behavior with CFD. *Biointerface Res. Appl. Chem.* **2020**, *10*, 7120–7134
15. ; Al-Adili, A.; Al-Amiery, A.A.; Takriff, M.S. The inhibition of mild steel corrosion in 0.5 M H_2SO_4 solution by N-phenethylhydrazinecarbothioamide (N-PHC). *J. Phys.: Conf. Ser.* **2021**, *1795*, 012009, https://doi.org/10.1088/1742-6596/1795/1/012009.
16. Al-Shafey, H.I.; Hameed, R.S.A.; Ali, F.A.; Aboul-Magd, A.E.-A.S.; Salah, M. Effect of expired drugs as corrosion inhibitors for carbon steel in 1M HCL solution. *Int. J. Pharm. Sci. Rev. Res* **2014**, *27*, 146-152.
17. Shukla, S.K.; Singh, A.K.; Ahamad, I.; Quraishi, M.A. Streptomycin: A commercially available drug as corrosion inhibitor for mild steel in hydrochloric acid solution. *Mater. Lett.* **2009**, *63*, 819-822, https://doi.org/10.1016/j.matlet.2009.01.020.
18. El-Naggar, M.M. Corrosion inhibition of mild steel in acidic medium by some sulfa drugs compounds. *Corros. Sci.* **2007**, *49*, 2226-2236, https://doi.org/10.1016/j.corsci.2006.10.039.
19. Qiang, Y.; Guo, L.; Li, H.; Lan, X. Fabrication of environmentally friendly Losartan potassium film for corrosion inhibition of mild steel in HCl medium. *Chem. Eng. J.* **2021**, *406*, 126863, https://doi.org/10.1016/j.cej.2020.126863.
20. Gupta, N.K.; Gopal, C.S.A.; Srivastava, V.; Quraishi, M.A. Application of expired drugs in corrosion inhibition of mild steel. *Int. J. Pharm. Chem. Anal.* **2017**, *4*, 8–12.
21. Singh, P.; Chauhan, D.S.; Srivastava, K.; Srivastava, V.; Quraishi, M.A. Expired atorvastatin drug as corrosion inhibitor for mild steel in hydrochloric acid solution. *Int. J. Ind. Chem.* **2017**, *8*, 363-372, https://doi.org/10.1007/s40090-017-0120-5.
22. Hameed, R.S.A. Ranitidine Drugs as Non-Toxic Corrosion Inhibitors for Mild Steel in Hydrochloric Acid Medium. *Port. Electrochim. Acta* **2011**, *29*, 273-285, http://dx.doi.org/10.4152/pea.201104273.
23. Srivastava, M.; Tiwari, P.; Srivastava, S.K.; Prakash, R.; Ji, G. Electrochemical investigation of Irbesartan drug molecules as an inhibitor of mild steel corrosion in 1 M HCl and 0.5 M H_2SO_4 solutions. *J. Mol. Liq.* **2017**, *236*, 184-197, https://doi.org/10.1016/j.molliq.2017.04.017.
24. Shukla, S.K.; Quraishi, M.A. Cefalexin drug: A new and efficient corrosion inhibitor for mild steel in hydrochloric acid solution. *Mater. Chem. Phys.* **2010**, *120*, 142-147, https://doi.org/10.1016/j.matchemphys.2009.10.037.
25. Fouda, A.S.; El-Ewady, G.; Ali, A.H. Modazar as promising corrosion inhibitor of carbon steel in hydrochloric acid solution. *Green Chem. Lett. Rev.* **2017**, *10*, 88-100, https://doi.org/10.1080/17518253.2017.1299228.
26. Alamry, K.A.; Khan, A.; Aslam, J.; Hussein, M.A.; Aslam, R. Corrosion inhibition of mild steel in hydrochloric acid solution by the expired Ampicillin drug. *Sci. Rep.* **2023**, *13*, 6724, https://doi.org/10.1038/s41598-023-33519-y.
27. Pour-Ali, S.; Hejazi, S. Tiazofurin drug as a new and non-toxic corrosion inhibitor for mild steel in HCl solution: Experimental and quantum chemical investigations. *J. Mol. Liq.* **2022**, *354*, 118886, https://doi.org/10.1016/j.molliq.2022.118886.
28. Kumar, S.H.; Karthikeyan, S. inhibition of mild steel corrosion in hydrochloric acid solution by cloxacillin drug. *J. Mater. Environ. Sci.* **2012**, *3*, 925–934.
29. Shojaee, S.; Shahidi Zandi, M.; Rastakhiz, N. The effect of Tetracycline drug as a green corrosion inhibitor for carbon steel in HCl media. *J. Indian Chem. Soc.* **2022**, *99*, 100700,

https://doi.org/10.1016/j.jics.2022.100700.
30. Fouda, A.S.; Eissa, M.; El-Hossiany, A. Ciprofloxacin as Eco-Friendly Corrosion Inhibitor for Carbon Steel in Hydrochloric Acid Solution. *Int. J. Electrochem. Sci.* **2018**, *13*, 11096-11112, https://doi.org/10.20964/2018.11.86.
31. Hameed, R.S.A.; AlShafey, H.I.; Abu-Nawwas, A.H. 2-(2, 6-dichloranilino) phenyl acetic acid Drugs as Eco-Friendly Corrosion Inhibitors for Mild Steel in 1M HCl. *Int. J. Electrochem. Sci.* **2014**, *9*, 6006-6019, https://doi.org/10.1016/S1452-3981(23)10865-0.
32. Matad, P.B.; Mokshanatha, P.B.; Hebbar, N.; Venkatesha, V.T.; Tandon, H.C. Ketosulfone Drug as a Green Corrosion Inhibitor for Mild Steel in Acidic Medium. *Ind. Eng. Chem. Res.* **2014**, *53*, 8436-8444, https://doi.org/10.1021/ie500232g.
33. Al-Fahemi, J.H.; Abdallah, M.; Gad, E.A.M.; Jahdaly, B.A.A.L. Experimental and theoretical approach studies for melatonin drug as safely corrosion inhibitors for carbon steel using DFT. *J. Mol. Liq.* **2016**, *222*, 1157-1163, https://doi.org/10.1016/j.molliq.2016.07.085.
34. Elgyar, O.A.; Ouf, A.M.; El-Hossiany, A.; Fouda, A.E.-A.S. The Inhibition Action of *Viscum Album* Extract on the Corrosion of Carbon Steel in Hydrochloric Acid Solution. *Biointerface Res. Appl. Chem.* **2021**, *11*, 14344–14358
35. Sasikumar, Y.; Adekunle, A.S.; Olasunkanmi, L.O.; Bahadur, I.; Baskar, R.; Kabanda, M.M.; Obot, I.B.; Ebenso, E.E. Experimental, quantum chemical and Monte Carlo simulation studies on the corrosion inhibition of some alkyl imidazolium ionic liquids containing tetrafluoroborate anion on mild steel in acidic medium. *J. Mol. Liq.* **2015**, *211*, 105-118, https://doi.org/10.1016/j.molliq.2015.06.052.
36. Fadhil, A.A.; Khadom, A.A.; Liu, H.; Fu, C.; Wang, J.; Fadhil, N.A.; Mahood, H.B. (S)-*6-Phenyl-2,3,5,6-tetrahydroimidazo[2,1-b] thiazole* hydrochloride as corrosion inhibitor of steel in acidic solution: Gravimetrical, electrochemical, surface morphology and theoretical simulation. *J. Mol. Liq.* **2019**, *276*, 503-518, https://doi.org/10.1016/j.molliq.2018.12.015.
37. Verma, C.; Olasunkanmi, L.O.; Obot, I.B.; Ebenso, E.E.; Quraishi, M.A. 2,4-Diamino-5-(phenylthio)-5*H*-chromeno [2,3-*b*] pyridine-3-carbonitriles as green and effective corrosion inhibitors: gravimetric, electrochemical, surface morphology and theoretical studies. *RSC Advances* **2016**, *6*, 53933-53948, https://doi.org/10.1039/C6RA04900A.
38. Melhi, S.; Bedair, M.A.; Alosaimi, E.H.; Younes, A.A.O.; El-Shwiniy, W.H.; Abuelela, A.M. Effective corrosion inhibition of mild steel in hydrochloric acid by newly synthesized Schiff base nano Co(II) and Cr(III) complexes: spectral, thermal, electrochemical and DFT (FMO, NBO) studies. *RSC Adv.***2022**, *12*, 32488-32507, https://doi.org/10.1039/D2RA06571A.
39. Chauhan, D.S.; Quraishi, M.A.; Qurashi, A. Recent trends in environmentally sustainable Sweet corrosion inhibitors. *J. Mol. Liq.* **2021**, *326*, 115117, https://doi.org/10.1016/j.molliq.2020.115117.
40. Fouda, A.S.; Abdel-Latif, E.; Helal, H.M.; El-Hossiany, A. Synthesis and Characterization of Some Novel Thiazole Derivatives and Their Applications as Corrosion Inhibitors for Zinc in 1 M Hydrochloric Acid Solution. *Russ. J. Electrochem.* **2021**, *57*, 159-171, https://doi.org/10.1134/S1023193521020105.
41. Huang, L.; Liu, W.; Shen, J.; Liao, Q. Study of antiviral drug Famciclovir as a corrosion inhibitor for carbon steel in hydrochloric acid medium. *Thin Solid Films* **2023**, *782*, 140005, https://doi.org/10.1016/j.tsf.2023.140005.
42. Narang, R.; Vashishth, P.; Bairagi, H.; Shukla, S.K.; Mangla, B. Electrochemical and surface study of an antibiotic drug as sustainable corrosion inhibitor on mild steel in 0.5 M H_2SO_4. *J. Mol. Liq.* **2023**, *384*, 122277, https://doi.org/10.1016/j.molliq.2023.122277.
43. Fouda, A.S.; Rashwan, S.; El-Hossiany, A.; El-Morsy, F.E. Corrosion inhibition of zinc in hydrochloric acid solution using some organic compounds as eco-friendly inhibitors. *J. Chem. Biol. Phys. Sci* **2019**, *9*, 1-24.
44. Abdallah, M.; Soliman, K.A.; Alfakeer, M.; Hawsawi, H.; Al-bonayan, A.M.; Al-Juaid, S.S.; Abd El Wanees, S.; Motawea, M.S. Expired Antifungal Drugs as Effective Corrosion Inhibitors for Carbon Steel in 1 M HCl Solution: Practical and Theoretical Approaches. ACS Omega 2023, 8, 34516-34533, https://doi.org/10.1021/acsomega.3c03257.
45. Iroha, N.B.; Anadebe, V.C.; Maduelosi, N.J.; Nnanna, L.A.; Isaiah, L.C.; Dagdag, O.; Berisha, A.; Ebenso, E.E. Linagliptin drug molecule as corrosion inhibitor for mild steel in 1 M HCl solution: Electrochemical, SEM/XPS, DFT and MC/MD simulation approach. *Colloids Surf. A: Physicochem. Eng. Asp.* **2023**, *660*, 130885, https://doi.org/10.1016/j.colsurfa.2022.130885.
46. Mehta, R.K.; Yadav, M. Corrosion inhibition properties of expired Broclear medicine and its carbon dot as eco-friendly inhibitors for mild steel in 15% HCl. *Mater. Sci. Eng. B* **2023**, *295*, 116566,

https://doi.org/10.1016/j.mseb.2023.116566.
47. Fouda, A.S.; El-Ghaffar, M.A.A.; Sherif, M.H.; El-Habab, A.T.; El-Hossiany, A. Novel Anionic 4-Tert-Octyl Phenol Ethoxylate Phosphate Surfactant as Corrosion Inhibitor for C-steel in Acidic Media. *Prot. Met. Phys. Chem. Surf.* **2020**, *56*, 189-201, https://doi.org/10.1134/S2070205120010086.
48. Wang, X.; Guo, H.; Cai, S.; Xu, X. Expired antihypertensive drugs as eco-friendly and efficient corrosion inhibitors for carbon steel in CO_2-saturated oilfield water: Experimental and theoretical approaches. *J. Mol. Struct.* **2023**, *1294*, 136555, https://doi.org/10.1016/j.molstruc.2023.136555.
49. Wang, Q.; Liu, L.; Zhang, Q.; Wu, X.; Zheng, H.; Gao, P.; Zeng, G.; Yan, Z.; Sun, Y.; Li, Z.; Li, X. Insight into the anti–corrosion performance of *Artemisia argyi leaves* extract as eco–friendly corrosion inhibitor for carbon steel in HCl medium. *Sustain. Chem. Pharm.* **2022**, *27*, 100710, https://doi.org/10.1016/j.scp.2022.100710.
50. Prabhu, R.A.; Venkatesha, T.V.; Shanbhag, A.V.; Kulkarni, G.M.; Kalkhambkar, R.G. Inhibition effects of some Schiff's bases on the corrosion of mild steel in hydrochloric acid solution. *Corros. Sci.* **2008**, *50*, 3356-3362, https://doi.org/10.1016/j.corsci.2008.09.009.
51. Fouda, A.E.S.; Motaal, S.M.A.; Ahmed, A.S.; Sallam, H.B.; Ezzat, A.; El-Hossiany, A. Corrosion protection of carbon steel in 2M HCl using aizoon canariense extract. *Biointerface Res. Appl. Chem.* **2021**, *12*, 230
52. Aljourani, J.; Raeissi, K.; Golozar, M.A. Benzimidazole and its derivatives as corrosion inhibitors for mild steel in 1M HCl solution. *Corros. Sci.* **2009**, *51*, 1836-1843, https://doi.org/10.1016/j.corsci.2009.05.011.
53. Durnie, W.; De Marco, R.; Jefferson, A.; Kinsella, B. Development of a Structure-Activity Relationship for Oil Field Corrosion Inhibitors. *J. Electrochem. Soc.* **1999**, *146*, 1751, https://doi.org/10.1149/1.1391837.
54. Khaled, K.F.; Hackerman, N. Investigation of the inhibitive effect of *ortho*-substituted anilines on corrosion of iron in 1 M HCl solutions. *Electrochim. Acta* **2003**, *48*, 2715-2723, https://doi.org/10.1016/S0013-4686(03)00318-9.
55. Yurt, A.; Bereket, G.; Kivrak, A.; Balaban, A.; Erk, B. Effect of Schiff Bases Containing Pyridyl Group as Corrosion Inhibitors for Low Carbon Steel in 0.1 M HCl. *J. Appl. Electrochem.* **2005**, *35*, 1025-1032, https://doi.org/10.1007/s10800-005-7336-3.
56. Sherif, E.M.; Park, S.-M. Inhibition of copper corrosion in acidic pickling solutions by *N*-phenyl-1,4-phenylenediamine. *Electrochim. Acta* **2006**, *51*, 4665-4673, https://doi.org/10.1016/j.electacta.2006.01.007.
57. El Faydy, M.; Touir, R.; Ebn Touhami, M.; Zarrouk, A.; Jama, C.; Lakhrissi, B.; Olasunkanmi, L.O.; Ebenso, E.E.; Bentiss, F. Corrosion inhibition performance of newly synthesized 5-alkoxymethyl-8-hydroxyquinoline derivatives for carbon steel in 1 M HCl solution: experimental, DFT and Monte Carlo simulation studies. *Phys. Chem. Chem. Phys.* **2018**, *20*, 20167-20187, https://doi.org/10.1039/C8CP03226B.
58. Gowraraju, N.D.; Jagadeesan, S.; Ayyasamy, K.; Olasunkanmi, L.O.; Ebenso, E.E.; Subramanian, C. Adsorption characteristics of Iota-carrageenan and Inulin biopolymers as potential corrosion inhibitors at mild steel/sulphuric acid interface. *J. Mol. Liq.* **2017**, *232*, 9-19, https://doi.org/10.1016/j.molliq.2017.02.054.
59. Etaiw, S.E.H.; Hassan, G.S.; El-Hossiany, A.A.; Fouda, A.S. Nano-metal–organic frameworks as corrosion inhibitors for strengthening anti-corrosion behavior of carbon steel in a sulfuric acid environment: from synthesis to applications. *RSC Adv.* **2023**, *13*, 15222-15235, https://doi.org/10.1039/D3RA01644G.
60. Fouda, A.S.; El-Maksoud, S.A.A.; Belal, A.A.M.; El-Hossiany, A.; Ibrahium, A. Effectiveness of Some Organic Compounds as Corrosion Inhibitors for Stainless Steel 201 in 1M HCl: Experimental and Theoretical Studies. *Int. J. Electrochem. Sci.* **2018**, *13*, 9826-9846, https://doi.org/10.20964/2018.10.36.
61. Ibrahim, M.B.; Sulaiman, Z.; Usman, B.; Ibrahim, M.A. Effect of Henna Leaves on the Corrosion Inhibition of Tin in Acidic and Alkaline Media. *World* **2019**, *4*, 45-51, http://dx.doi.org/10.11648/j.wjac.20190404.11.
62. Ostovari, A.; Hoseinieh, S.M.; Peikari, M.; Shadizadeh, S.R.; Hashemi, S.J. Corrosion inhibition of mild steel in 1M HCl solution by henna extract: A comparative study of the inhibition by henna and its constituents (Lawsone, Gallic acid, α-d-Glucose and Tannic acid). *Corros. Sci.* **2009**, *51*, 1935-1949, https://doi.org/10.1016/j.corsci.2009.05.024.
63. Devi, P.N.; Sathiyabama, J.; Rajendran, S. Study of surface morphology and inhibition efficiency of mild steel in simulated concrete pore solution by lactic acid–Zn^{2+} system. *Int. J. Corros. Scale Inhib* **2017**, *6*, 18-31, http://dx.doi.org/10.17675/2305-6894-2017-6-1-2.
64. Habibiyan, A.; Ramezanzadeh, B.; Mahdavian, M.; Kasaeian, M. Facile size and chemistry-controlled synthesis of mussel-inspired bio-polymers based on Polydopamine Nanospheres: Application as eco-friendly corrosion inhibitors for mild steel against aqueous acidic solution. *J. Mol. Liq.* **2020**, *298*, 111974, https://doi.org/10.1016/j.molliq.2019.111974.

65. Refat, H.M.; Fadda, A.A. Synthesis and Antimicrobial Activity of Some Novel Hydrazide, Pyrazole, Triazine, Isoxazole, and Pyrimidine Derivatives. *J. Heterocycl. Chem* **2016**, *53*, 1129-1137, https://doi.org/10.1002/jhet.2369.
66. Fouda, A.S.; Ahmed, R.E.; El-Hossiany, A. Chemical, Electrochemical and Quantum Chemical Studies for Famotidine Drug as a Safe Corrosion Inhibitor for α-Brass in HCl Solution. *Prot. Met. Phys. Chem. Surf.* **2021**, *57*, 398-411, https://doi.org/10.1134/S207020512101010X.
67. Kumar, R.; Yadav, O.S.; Singh, G. Electrochemical and surface characterization of a new eco-friendly corrosion inhibitor for mild steel in acidic media: A cumulative study. *J. Mol. Liq.* **2017**, *237*, 413-427, https://doi.org/10.1016/j.molliq.2017.04.103.
68. Fouda, A.S.; Ibrahim, H.; Rashwaan, S.; El-Hossiany, A.; Ahmed, R.M. Expired Drug (pantoprazole sodium) as a Corrosion Inhibitor for High Carbon Steel in Hydrochloric Acid Solution. *Int. J. Electrochem. Sci.* **2018**, *13*, 6327-6346, https://doi.org/10.20964/2018.07.33.
69. Fouda, A.S.; Etaiw, S.E.H.; Ibrahim, A.M.; El-Hossiany, A.A. Insights into the use of two novel supramolecular compounds as corrosion inhibitors for stainless steel in a chloride environment: experimental as well as theoretical investigation. *RSC Adv.* **2023**, *13*, 35305-35320, https://doi.org/10.1039/D3RA07397A.
70. Fouda, A.E.-A.S.; Etaiw, S.E.H.; Abd El-Aziz, D.M.; El-Hossiany, A.A.; Elbaz, U.A. Experimental and theoretical studies of the efficiency of metal–organic frameworks (MOFs) in preventing aluminum corrosion in hydrochloric acid solution. *BMC Chem.* **2024**, *18*, 21, https://doi.org/10.1186/s13065-024-01121-6.
71. Eissa, M.; Etaiw, S.H.; El-Waseef, E.E.; El-Hossiany, A.; Fouda, A.S. The impact of environmentally friendly supramolecular coordination polymers as carbon steel corrosion inhibitors in HCl solution: synthesis and characterization. *Sci. Rep.* **2024**, *14*, 2413, https://doi.org/10.1038/s41598-024-51576-9.
72. Rajendran, S.; Thangavelu, C.; Annamalai, G. Inhibition of corrosion of aluminium in alkaline medium by succinic acid in conjunction with zinc sulphate and diethylene triamine penta (Methylene phosphonic acid). *J. Chem. Pharm. Res.* **2012**, *4*, 4836-4844.
73. El Basiony, N.M.; Elgendy, A.; Nady, H.; Migahed, M.A.; Zaki, E.G. Adsorption characteristics and inhibition effect of two Schiff base compounds on corrosion of mild steel in 0.5 M HCl solution: experimental, DFT studies, and Monte Carlo simulation. *RSC Adv.* **2019**, *9*, 10473-10485, https://doi.org/10.1039/C9RA00397E.
74. Khaled, M.A.; Ismail, M.A.; El-Hossiany, A.A.; Fouda, A.E.-A.S. Novel pyrimidine-bichalcophene derivatives as corrosion inhibitors for copper in 1 M nitric acid solution. *RSC Adv.* **2021**, *11*, 25314-25333, https://doi.org/10.1039/d1ra03603c.
75. Odewole, O.A.; Ibeji, C.U.; Oluwasola, H.O.; Oyeneyin, O.E.; Akpomie, K.G.; Ugwu, C.M.; Ugwu, C.G.; Bakare, T.E. Synthesis and anti-corrosive potential of Schiff bases derived 4-nitrocinnamaldehyde for mild steel in HCl medium: Experimental and DFT studies. *J. Mol. Struct.* **2021**, *1223*, 129214, https://doi.org/10.1016/j.molstruc.2020.129214.
76. Fouda, A.S.; Ismail, M.A.; Khaled, M.A.; El-Hossiany, A.A. Experimental and computational chemical studies on the corrosion inhibition of new pyrimidinone derivatives for copper in nitric acid. *Sci. Rep.* **2022**, *12*, 16089, https://doi.org/10.1038/s41598-022-20306-4.
77. Khaled, K.F.; El-Maghraby, A. Experimental, Monte Carlo and molecular dynamics simulations to investigate corrosion inhibition of mild steel in hydrochloric acid solutions. *Arab. J. Chem.* **2014**, *7*, 319-326, https://doi.org/10.1016/j.arabjc.2010.11.005.
78. Fouda, A.S.; Abdel-Wahed, H.M.; Atia, M.F.; El-Hossiany, A. Novel porphyrin derivatives as corrosion inhibitors for stainless steel 304 in acidic environment: synthesis, electrochemical and quantum calculation studies. *Sci. Rep.* **2023**, *13*, 17593, https://doi.org/10.1038/s41598-023-44873-2.
79. Ammouchi, N.; Allal, H.; Belhocine, Y.; Bettaz, S.; Zouaoui, E. DFT computations and molecular dynamics investigations on conformers of some pyrazinamide derivatives as corrosion inhibitors for aluminum. *J. Mol. Liq.* **2020**, *300*, 112309, https://doi.org/10.1016/j.molliq.2019.112309.
80. El Hamdani, N.; Fdil, R.; Tourabi, M.; Jama, C.; Bentiss, F. Alkaloids extract of *Retama monosperma* (L.) Boiss. seeds used as novel eco-friendly inhibitor for carbon steel corrosion in 1M HCl solution: Electrochemical and surface studies. *Appl. Surf. Sci.* **2015**, *357*, 1294-1305, https://doi.org/10.1016/j.apsusc.2015.09.159.
81. Boumhara, K.; Tabyaoui, M.; Jama, C.; Bentiss, F. *Artemisia Mesatlantica* essential oil as green inhibitor for carbon steel corrosion in 1M HCl solution: Electrochemical and XPS investigations. *J. Ind. Eng. Chem.* **2015**, *29*, 146-155, https://doi.org/10.1016/j.jiec.2015.03.028.

82. Fouda, A.S.; Shalabi, K.; E-Hossiany, A. Moxifloxacin Antibiotic as Green Corrosion Inhibitor for Carbon Steel in 1 M HCl. *J. Bio- Tribo-Corros.* **2016**, *2*, 18, https://doi.org/10.1007/s40735-016-0048-x.
83. Almzarzie, K.; Falah, A.; Massri, A.; Kellawi, H. Electrochemical impedance spectroscopy (EIS) and study of iron corrosion inhibition by turmeric roots extract (TRE) in hydrochloric acid solution. *Egypt. J. Chem.* **2019**, *62*, 501-512, https://doi.org/10.21608/ejchem.2018.5295.1476.
84. Soltani, N.; Tavakkoli, N.; Attaran, A.; Karimi, B.; Khayatkashani, M. Inhibitory effect of *Pistacia khinjuk* aerial part extract for carbon steel corrosion in sulfuric acid and hydrochloric acid solutions. *Chem. Pap.* **2020**, *74*, 1799-1815, https://doi.org/10.1007/s11696-019-01026-y.